Solar Physics
DOI: 10.1007/•••••-•••-•••-••••-•

Unusual Solar Radio Burst Observed at Decameter Wavelengths

V.N. Melnik[1] · **A.I. Brazhenko**[2] · **A.A. Konovalenko**[1] · **H.O. Rucker**[3] · **A.V. Frantsuzenko**[2] · **V.V. Dorovskyy**[1] · **M. Panchenko**[3] · **A.A. Stanislavskyy**[1]

Abstract An unusual solar burst was observed simultaneously by two decameter radio telescopes UTR-2 (Kharkov, Ukraine) and URAN-2 (Poltava, Ukraine) on 3 June 2011 in the frequency range 16-28 MHz. The observed radio burst has some unusual properties, which are not typical for the other types of solar radio bursts. The frequency drift rate of it was positive (about 500 kHz s^{-1}) at frequencies higher than 22 MHz and negative (100 kHz s^{-1}) at lower frequencies. The full duration of this event varies from 50 s up to 80 s, depending on the frequency. The maximum radio flux of the unusual burst reaches $\approx 10^3$ s.f.u and its polarization does not exceed 10%. This burst has a fine frequency-time structure of unusual appearance. It consists of stripes with the frequency bandwidth 300-400 kHz. We consider that several accompanied radio and optical events observed by SOHO and STEREO spacecraft are possibly associated with the reported radio burst. A model that may interpret the observed unusual solar radio burst is proposed.

Keywords: Solar radio bursts, Plasma mechanism of radio emission, Harmonic radio emission, Decameter radio telescope, Polarization

1. Introduction

Sporadic radio emission of the Sun is observed all over the wavelength band, from millimeter to kilometer wavelengths (Suzuki and Dulk, 1985). The observed frequencies of some types of radio bursts such as type II and type III bursts as

[1] Institute of Radio Astronomy, National Academy of Sciences of Ukraine, Kharkov, Ukraine email: melnik@ri.kharkov.ua
[2] Gravimetrical Observatory, National Academy of Sciences of Ukraine, Poltava, Ukraine email: brazhai@gmail.com
[3] Space Research Institute, Austrian Academy of Sciences, Graz, Austria email: mykhaylo.panchenko@oeaw.ac.at email: rucker@oeaw.ac.at

well as S-bursts drift from high to low frequencies, whereas other radio emissions, *i.e.* type IV radio bursts, are recorded simultaneously in a wide frequency range from decimeter to decameter wavelengths. On the other hand narrow and short spikes of emission are observed independently at decimeter, meter, and decameter wavelengths.

In the decameter range the following types of sporadic solar radio emission are observed

- type III bursts (Abranin *et al.*, 1980; Melnik *et al.*, 2005b) and, related to them, type IIIb bursts (Bazelian, Zinichev, and Rapoport, 1978; Melnik *et al.*, 2010c);
- ordinary type II bursts and type II bursts with herringbone structure (Melnik *et al.*, 2004);
- type IV bursts (Melnik *et al.*, 2008b);
- inverted U- and J- bursts (Dorovsky *et al.*, 2010);
- S-bursts (Dorovskyy *at al.*, 2006; Briand *at al.*, 2008; Melnik *at al.*, 2010b);
- drift pairs (Melnik *et al.*, 2005a);
- short and extended bursts in absorption (Konovalenko *et al.*, 2007; Melnik *et al.*, 2010a).

The decameter radio telescopes with large effective areas such as UTR-2 equipped with spectrometers operating in a broad frequency band have discovered fast type III bursts (Melnik *et al.*, 2008a), dog-leg type III bursts (Dorovskyy *et al.*, 2011), and decameter spikes (Melnik *et al.*, 2011). Moreover the modern back-end facilities with high time-frequency resolution allowed us to study the properties of fine temporal structure of type II and III bursts (Melnik *et al.*, 2004, 2005a) and zebra structure of type IV bursts (Melnik *et al.*, 2008b) in details.

The main parameters of the solar radio bursts are the frequency band width, frequency drift rate, duration, polarization degree, and flux of the radio emission. This set of parameters allows us to classify radio bursts. For example, a typical frequency drift rate of the usual (not fast) type III bursts in the decameter range is 2-4 MHz s^{-1}, whereas type II bursts have frequency drift rates about 30-70 kHz s^{-1} (Melnik *et al.*, 2004). The duration of type III bursts in the decameter band is 6-12 s (Abranin *et al.*, 1980; Melnik *et al.*, 2005b). Type IV bursts are observed during an interval from 1-1.5 h to several hours (Melnik *et al.*, 2008b), whereas S-bursts have duration of only 0.3-0.6 s. The frequency drift rate of S-bursts is about 1 MHz s^{-1} (Melnik *et al.*, 2010b).

The sources of radio emission for different types of bursts are fast particles (in most cases, electrons), which propagate through different magnetic structures in the solar corona (Suzuki and Dulk, 1985). Fast electrons accelerated during flares and moving along open the magnetic field lines are responsible for type III bursts. Electrons accelerated at shock fronts generate type II radio bursts. Radio emission of type IV bursts is a result of interaction between CME and plasma of the solar corona.

In this paper we report the observation of an unusual solar radio burst. This burst was recorded simultaneously by two Ukrainian decameter radio telescopes, UTR-2 (Kharkov, Ukraine) and URAN-2 (Poltava, Ukraine) on 3 June 2011. The observed solar radio burst cannot be referred to any known type of the bursts in the decameter range. We discuss the properties of this burst and consider

the associated radio and plasma phenomena observed simultaneously by SOHO and STEREO. A model or possible scenario of the unusual burst generation is proposed.

2. Observations of Unusual Decameter Solar Radio Burst

An unusual burst in the form of a "caterpillar" was observed during a decameter type III storm at 12:10 on 3 June 2011. This burst was observed simultaneously by UTR-2 and URAN-2 radio telescopes. During this observation the UTR-2 radio telescope was operated in the mode in which only four sections of the north-south branch of the antenna was used. The total effective area of these four sections was 50000 m^2 with the beam pattern size of $1^\circ \times 15^\circ$ at 25 MHz. The radio telescope URAN-2 (Poltava, Ukraine) has the effective area of 28000 m^2 and its beam pattern size is $3.5^\circ \times 7^\circ$ at 25 MHz (Megn *et al.*, 2003; Brazhenko *et al.*, 2005). Additionally URAN-2 is able to measure the degree of polarization of the received radio signal. The data were recorded by the digital DSP spectrometers (Ryabov *et al.*, 2010) operating in the frequency range of 16-32 MHz with a frequency-time resolution of $4\,\mathrm{kHz} \times 100\,\mathrm{ms}$.

Figure 1 shows the dynamic radio spectra obtained by URAN-2 (panel a) and UTR-2 (panel b). The unusual burst was observed at around 12:10 UT at the frequencies from $\approx$ 16 MHz to $\approx$ 27.5 MHz. This burst was recorded simultaneously by UTR-2 and URAN-2 radio telescopes and the obtained radio spectra look identically.

High frequency-time resolution of the radio telescopes gives an opportunity to observe a complex fine structure of the unusual burst as shown in Figure 2. The burst consisted of 14 narrow-band stripes of different duration. Comparing this stripe structure with known striae fine features of type IIIb bursts we can find significant differences. In particular, the frequency bandwidth of the stripes of the unusual burst is about 300-400 kHz whereas the striae of type IIIb bursts in the decameter range have narrower bandwidth, only 50-70 kHz (Melnik *et al.*, 2011). The second difference is that individual stria of type IIIb present a straight track whereas the stripes of unusual burst looked like a serpentine.

The caterpillar exhibited negative and positive frequency drifts simultaneously. In particular, the frequency drift rate of the burst was positive (about 500 kHz s^{-1}) at frequencies higher than 22 MHz and negative (100 kHz s^{-1}) at lower frequencies. These frequency drift rates are lower than those for type III bursts but higher than typical drift rates for type II bursts in the decameter range. The maximum flux of the unusual radio burst did not exceed 10^3 s.f.u.

The very interesting feature of the caterpillar is its strong cut-off at high frequencies. As shown in Figure 1 the burst abruptly disappeared at 27.5 MHz. At the same time there was no cut-off at low frequencies and the burst was observed by STEREO significantly below 16 MHz (see Figure 5).

The time profile of the unusual burst at 26 MHz is shown in Figure 3. Contrary to type III bursts the time profile of the unusual burst had a bell-like shape. The full duration of the burst varied from 50 s at lower frequencies to 80 s at frequencies above 22 MHz. Such durations are significantly larger than the

average durations of individual type III bursts at decameter wavelengths, namely 6-12 s.

Figure 4 shows the time profile of the polarization measurements at a frequency of 26 MHz. The polarization degree of the caterpillar was practically constant and was $\approx 10\%$. Such a degree of polarization is typical for the second harmonic of type III bursts (Dulk and Suzuki, 1980). This give us an idea that if the generation mechanism of the unusual burst is similar to those for type III bursts, then the unusual burst was radiated at the second harmonic.

Additional to the ground-based observations we have also examined the data recorded by radio experiment WAVES onboard two STEREO spacecraft (STEREO-A and STEREO-B; Bougeret *at al.*, 2008). On 3 June 2011 two spacecraft were located on the heliocentric orbits with angular separation $\approx 180°$, *i.e.* on the opposite sides of the Sun (see Figure 5b). The dynamic radio spectra recorded by STEREO-A and STEREO-B in the frequency range from 1 MHz to 16 MHz are shown in Figure 5a. As is seen, only one spacecraft, STEREO-A, observed the unusual burst at $\approx$ 12:10 UT. STEREO-B recorded only a group of type III bursts at frequencies lower than 2 MHz at around 12:04 UT, which was also well visible in the UTR-2 and URAN-2 spectra (see Figure 1). Taking into account the positions of STEREO-A and STEREO-B (Figure 5b) we conclude that the source of the unusual burst was situated on the west side of the Sun with respect to the Earth. We have also estimated the frequency drift rate of the unusual burst observed by STEREO-A at frequencies 1-16 MHz. This drift rate was about 50 kHz s^{-1} which was smaller than typical drift rates of type III bursts at these frequencies (see, for example, a group of type III bursts at 12:04 in Figure 5a).

3. Observations of Accompanied Phenomena

After detection of the caterpillar (at 12:10 UT) two coronagraphs LASCO C2 and C3 onboard SOHO have observed three phenomena on the west side of the solar disk (Figure 6). In particular LASCO C2 recorded two successive ejections appeared at 12:48 and 13:36 UT. The sizes of these two ejections were smaller than the typical size of coronal mass ejections (CMEs). At 12:48 there was also a jet at a latitude higher than those of the ejections (Figure 6). According to UV images from SOHO (Figure 7a) no active regions were detected on the west side of the solar disk. At the same time STEREO-A/EUVI observed two active regions NOAA 1224 and NOAA 1222 situated at approximately 100° and $130° - 140°$ of western longitude with respect to the central meridian (Figure 7b). Since NOAA 1222 was on the lower latitude than the active region NOAA 1224 we may consider that NOAA 1222 initiated two ejections while the NOAA 1224 triggered the jet.

In order to clarify which of the ejections or the jet observed by SOHO (Figure 6) were related to the unusual burst, let us consider how the ejections and jet propagated. Figures 8 and 9 present the motions of two ejections as well as the front of the jet according to LASCO C2 and LASCO C3 observations. From LASCO C2 observations the front $r_{\mathrm{f,p}}$ and the center $r_{\mathrm{c,p}}$ of the first ejection moved in the plane of the sky as

$$r_{\mathrm{f,p}} = 2.95 \times 10^{-2} \cdot t + 1.79 \quad (1)$$

$$r_{\mathrm{c,p}} = 2.91 \times 10^{-2} \cdot t + 1.45 \quad (2)$$

where r is the radial distance in units of the solar radius R_{s} , and t is the time in minutes counted from 12:10 UT. At the same time according to LASCO C3 data this propagation can be described as:

$$r_{\mathrm{f,p}} = 2.43 \times 10^{-2} \cdot t + 1.89 \quad (3)$$

$$r_{\mathrm{c,p}} = 2.55 \times 10^{-2} \cdot t + 1.003. \quad (4)$$

The above equations as well as the following (Equations (5) – (13)) are valid in the plane of the sky.

The linear velocities of the front and the center of the first ejection derived from the above equations are, respectively, 344 km s^{-1} and 340 km s^{-1} near the Sun (LASCO C2) and 284 km s^{-1} and 298 km s^{-1} far from the Sun (LASCO C3). It is seen that the first ejection decelerated with the distance, particularly the front of the ejection $r_{\mathrm{f,p}}$ decelerated faster than the ejection center $r_{\mathrm{c,p}}$. At 12:10, when the unusual burst started at a frequency of 22 MHz, the front of the first ejection was at $1.8R_{\mathrm{s}}$ and $1.9R_{\mathrm{s}}$ from the center of the Sun in the plane of the sky according to LASCO C2 and C3 respectively. Taking into account that this ejection was initiated by active region NOAA 1222 with a longitudinal angle $\alpha = 40^{\circ} - 50^{\circ}$ (α is defined in Figure 13), the real radial distance from the front of the ejection to the center of the Sun was $2.25 - 2.55R_{\mathrm{s}}$ (for $\alpha = 40^{\circ}$) or $2.35 - 2.69R_{\mathrm{s}}$ (for $\alpha = 50^{\circ}$). At the same time the radio emission of the unusual burst appeared firstly on the spectra at 22 MHz (at about 12:09:45 UT). Assuming that this radio emission was generated at the second harmonic of the local plasma frequency and using the models of Newkirk (1961) and Baumbach-Allen (Allen, 1947) we can estimate that the radio source should be at $r = 2.8R_{\mathrm{s}}$ and $r = 2.15R_{\mathrm{s}}$, respectively, in these models. Therefore we may suggest that the first ejection was very close to the place from which the radio emission of the unusual burst came out.

Equations which define the motion of the front $r^{(2)}_{\mathrm{f,p}}$ and the center $r^{(2)}_{\mathrm{c,p}}$ of the second ejection according to LASCO C2 observations are the following:

$$r^{(2)}_{\mathrm{f,p}} = 2.67 \times 10^{-2} \cdot t + 0.19 \quad (5)$$

$$r^{(2)}_{\mathrm{c,p}} = 2.81 \times 10^{-2} \cdot t - 0.29 \quad (6)$$

and according to LASCO C3 data:

$$r^{(2)}_{\mathrm{f,p}} = 2.37 \times 10^{-2} \cdot t + 0.39 \quad (7)$$

$$r^{(2)}_{\mathrm{c,p}} = 2.61 \times 10^{-2} \cdot t - 0.66. \quad (8)$$

Velocities (in the sky plane) of the front and the center of the second ejection were 311 km s^{-1} and 328 km s^{-1} (according to LASCO C2) and 277 km s^{-1} and 305 km s^{-1} (according to LASCO C3). For the second ejection the velocities of the front and the center of the ejection decreased with distance but only at the vicinity of the Sun, whereas far from the Sun the center moved faster than the front. As follows from Equations (5) – (8) and Figure 8 the second ejection reached the estimated heights in the corona ($2.15 - 2.8\,R_{\rm s}$) in 80-90 min after the beginning of the unusual burst. Therefore we can conclude that this ejection did not cause the unusual radio burst.

The jet front propagated through the solar corona with a constant velocity of about 265 km s^{-1} as seen in Figure 9 (taking into account the longitudinal angle $\alpha = 10^{\circ}$ of the active region NOAA 1224 which was supposed to associate with the jet). The equation which describes the motion of the jet front in the sky plane is:

$$r^{\rm j}_{\rm f,p} = 2.25 \times 10^{-2} \cdot t + 2.27. \tag{9}$$

The distance from the front of the jet to the center of the Sun at the time of the unusual radio burst was $2.3R_{\rm s}$. This radial distance is close to those at which the radio emission at the second harmonic at 22 MHz can be generated. Therefore the jet can be a source of the unusual radio burst too. Nevertheless we suggest that the unusual burst was connected with the first ejection because in this case some properties of the burst can be explained easier.

Further we need to know the size of the first ejection at the time of the unusual burst radiation. Figure 10 shows the dependence of the longitudinal (l) and the transverse (d) sizes of the ejection on the distance from the Sun according to LASCO C2 and C3 data. These dependencies for LASCO C2 data can be formulated as follows:

$$l_{\rm p} = 0.57 \times 10^{-2} \cdot t + 0.37 \tag{10}$$

$$d_{\rm p} = 0.15 \times 10^{-2} \cdot t + 0.26 \tag{11}$$

and out of LASCO C3 observations

$$l_{\rm p} = 0.3 \times 10^{-2} \cdot t + 0.63 \tag{12}$$

$$d_{\rm p} = 0.21 \times 10^{-2} \cdot t + 0.2. \tag{13}$$

The velocity estimated from the longitudinal extension of the ejection is υ_l = 66.5 km s^{-1} which is four times larger than the velocity derived from the transverse extension (υ_d = 17.5 km s^{-1}) in the vicinity of the Sun, whereas far from the Sun υ_l = 35 km s^{-1} and υ_d = 24.5 km s^{-1}. The expansion velocities of the first ejection were smaller than the bulk velocity. Therefore we can conclude that the density of the ejecta practically did not change during its movement. Such situation is possible when the surface magnetic field of the ejecta restrains plasma from expanding into the surrounding coronal plasma. Thus further we consider the ejection as a magnetic flux rope.

4. Model of Unusual Burst

We suppose that the magnetic flux rope was connected to the active region NOAA 1222. As it follows from STEREO-A/EUVI observations this region showed very high activity beginning from 11:36 UT. It manifested in increasing its brightness and size as well as in the appearance of arches related to this region. These processes lasted for about 2 h. Supposing that the magnetic flux rope moved radially from the active region with the longitude angle α and using Equations (1) and (2) we derive the following equations which describe the motions of the front $r_{\rm f}$ and center $r_{\rm c}$ of the ejection

$$r_{\rm f} = (2.95 \times 10^{-2} \cdot t + 1.79) \cos^{-1} \alpha \tag{14}$$

$$r_{\rm c} = (2.91 \times 10^{-2} \cdot t + 1.45) \cos^{-1} \alpha. \tag{15}$$

The magnetic flux rope was formed approximately at 11:36 UT (at the very beginning of NOAA 1222 activity) at longitudes $\alpha = 40^\circ - 50^\circ$ (according to Equation (14), $t = -34$ min) near the surface of the Sun. The central part of the flux rope appeared in 6 min, *i.e.* at 11:42 UT. According to Equation (10) and taking into account the angle $\alpha = 40^\circ - 50^\circ$ the longitudinal size of the magnetic flux rope was $l \approx 0.17 R_{\rm s}$ at the time of its formation. Velocities of its front and center were, respectively, 450 km s^{-1} and 443 km s^{-1} at $\alpha = 40^\circ$ and 535 km s^{-1} and 528 km s^{-1} at $\alpha = 50^\circ$. The ejection front was located at $R = 1.8 R_{\rm s}/\cos\alpha = 2.22 - 2.55 R_{\rm s}$ from the center of the Sun at the beginning of the unusual burst, *i.e.* at 12:10 UT (see Figure 11). As was discussed in Section 3, at these heights the local plasma frequency is about 11 MHz. Therefore the magnetic flux rope at these altitudes can be a source of radio emission at the second harmonic, 22 MHz.

Langmuir waves required for the generation of the radio emission through the plasma mechanism can be excited by electrons which are accelerated during the interaction of the moving magnetic flux rope with the surrounding coronal plasma. In the case when the magnetic field of the flux rope was perpendicular to the rope axis the electrons can be accelerated along the flux rope, for example, by the Lorentz force $\mathbf{F}_{\rm L} = \frac{e}{c} \mathbf{v}_d \times \mathbf{B}_r$, where $\mathbf{v}_d$ is the transverse velocity of the magnetic flux rope and $\mathbf{B}_r$ is the magnetic field of the flux rope (see Figure 12a). The other possible acceleration process is magnetic reconnection (Figure 12b) when the magnetic field of the flux rope was oriented along the direction of the propagation of the flux rope. At the constant acceleration along the flux rope the electrons can reach the velocity $\upsilon \approx 2L/\Delta t$, where L is the length of the flux rope and Δt is the acceleration time.

Assuming that the acceleration time is approximately equal to the duration of the unusual radio burst and taking into account that the length of the flux rope is $\approx 0.5 R_{\rm s}$ at radial distances of $R = 2.22 - 2.55 R_{\rm s}$ we can estimate the velocities of fast electrons as $\upsilon = 0.8 - 1.4 \cdot 10^9$ cm s^{-1}. These electrons can propagate towards and away from the Sun. Electrons moving through the coronal plasma generate Langmuir waves l which in the process $l + i = t + i$ (i means ion) are transformed into electromagnetic waves t at the first harmonic. In the process $l + l = t$ the

Langmuir waves are merged into electromagnetic waves at the second harmonic (Ginzburg and Zhelezniakov, 1958). The radio emission at the first harmonic generated in a behind-the-limb region cannot propagate toward the Earth. At the same time the second harmonic of the behind-the-limb radio emission can be observed on the Earth (see the Appendix). In the Newkirk model of coronal density, the radio emission at the second harmonic has a strong cut-off at the frequency f^* (see Equation (22)). For the active regions with the longitudinal angle $\alpha = 42^\circ$ this frequency is $f^* = 27.5$ MHz. It is the same frequency at which the unusual radio burst had a clear cut-off (see Figure 1).

We propose the following explanation of this cut-off of the caterpillar burst at 27.5 MHz. Electrons which were accelerated by the magnetic flux rope at $R = 2.22 - 2.55R_\mathrm{s}$ towards the Sun generate the radio emission of the unusual burst which drifted from 22 MHz up to 27.5 MHz. The radio emission could not propagate through the solar corona in the direction to the Earth at frequencies $f > 27.5$ MHz. At the same time electrons accelerated by the magnetic flux rope away from the Sun produced the radio emission of the unusual burst which drifted to low frequencies from 22 MHz to 16 MHz (according data of UTR-2 and URAN-2) and down to 1 MHz (according to the STEREO A data).

4.1. Frequency Drift Rate of the Unusual Burst

As was mentioned in Section 2, one of the interesting properties of the caterpillar burst is its unusual frequency drift. In particular, the frequency drift was positive at frequencies higher than 22 MHz and its rate was about 500 MHz s^{-1}, whereas at frequencies lower than 22 MHz the unusual burst exhibited negative frequency drift with the rate of about 100 MHz s^{-1}.

The particles accelerated by the flux rope may produce the radio emission which will be observed with the following frequency drift rate

$$\frac{df}{dt} = \frac{df}{dn} \cdot \frac{dn}{dr} \cdot \frac{\upsilon_\mathrm{s} c}{c - \upsilon_\mathrm{s} \cos\alpha}, \tag{16}$$

where υ_s is the electron velocity, c is the speed of light, and n is the plasma density. Using the Newkirk model we derive from Equation (16) in the case of the second harmonic of radio emission the following values for the electron velocities: $\upsilon_\mathrm{s} = 0.4 \cdot 10^9$ cm s^{-1} and $\upsilon_\mathrm{s} = 1.8 \cdot 10^9$ cm s^{-1} for the observed drift rates $\frac{df}{dt} = 100$ kHz s^{-1} and $\frac{df}{dt} = 500$ kHz s^{-1}, respectively. These velocities are close to those obtained for the acceleration of electrons by the magnetic flux rope.

4.2. Inhomogeneities of Coronal Plasma

Our observations showed a fine structure of the unusual burst in the form of stripes (Figure 2). These stripes had a longer duration than the striae of type IIIb bursts. Their frequency bandwidths are 6-8 times broader than the bandwidths of striae, *i.e.* 300-400 kHz for the unusual radio burst contrary to 50-70 kHz bandwidth of the type IIIb stria (Melnik *et al.*, 2010c). Additionally in contrast

to type IIIb bursts with a nearly constant frequency drift of the striae, the drift rate of the unusual burst stripes changed during the stripe (Figure 2).

We believe that the discussed stripes were related to an inhomogeneity of coronal plasma. This idea is analogous to the hypothesis proposed by Takakura and Yousef (1975) according to which the type IIIb stria radio emission may be explained as an amplification of the radio emission by irregularities in the solar corona, for example, by the filaments.

Kontar (2001) has considered the propagation of the fast electron beams in a plasma with density fluctuations and has shown that the Langmuir turbulence generated by electrons is higher in the low plasma density regions. Therefore, we can also expect more intense radio emission at regions of low density. The size of inhomogeneties which are responsible for the enhancement of the radio stripes of the unusual burst can be derived from the frequency bandwidth defined by

$$\Delta f \approx \frac{1}{\pi}\frac{d\omega_{\rm pe}}{dn}\frac{dn}{dr}\cdot\Delta r \approx \frac{1}{2n}\frac{dn}{dr}f\cdot\Delta r. \tag{17}$$

From Equation (17) we obtain the following size of inhomogeneities $\Delta r \approx \Delta f \cdot R_{\rm s}/f \approx 10^{-2}R_{\rm s}$. Thus we can conclude that the electron beams propagate through essentially non-homogeneous plasma. Note that an analogous result was derived for wide-band fibers, the fine structure elements of decameter type II bursts (Chernov *et al.*, 2007).

4.3. Brightness Temperature of the Unusual Radio Burst

Proposing that the radio emission of the unusual burst was generated by the particles accelerated by the magnetic flux rope it is reasonable to accept that the transverse size d of the volume of the accelerated particles is equal to the transverse size of the magnetic flux rope at the radial distances from which the radio emission comes out. From Equation (11) we derive that $d \approx 0.2R_{\rm s}$. Taking into account that the maximum flux of the unusual burst was about $F = 10^3$ s.f.u. (1 s.f.u. = 10^{-22} W m^{-2} Hz^{-1}) the corresponding brightness temperature is

$$T_{\rm b} = \frac{\lambda^2 F}{2k\Omega} \approx 10^{12}\ K \tag{18}$$

at the frequency $f = 22$ MHz and for the solid angle $\Omega = \pi d^2/4R_{\rm SE}^2 = 0.7\cdot10^{-6}$, where k is the Boltzman constant and $R_{\rm SE}$ is the distance from the Sun to the Earth. Such a high brightness temperature can be explained in the frame of plasma mechanism of radio emission (Melnik and Kontar, 2003).

5. Conclusions

The unusual burst observed by radio telescopes UTR-2 and URAN-2 at frequencies 16-27 MHz had the following properties:

1. Radio emission came out from a behind-the-limb region.

2. The burst has some unusual properties which are not typical for other known solar bursts. In particular,
   - the frequency drift rate was negative at low frequencies and positive at high frequencies;
   - the frequency drift rate changed in the range from 100 kHz s^{-1} to 500 kHz s^{-1};
   - the burst disappeared at frequencies > 27.5 MHz, *i.e.* it showed strong frequency cut-off effect;
   - the total duration of the burst (50 s - 80 s) was longer than that for the usual type III bursts;
   - the burst had a fine structure in the form of stripes with frequency bandwidth $300 - 400$ kHz;
3. The polarization of the burst was about 10%, which corresponded to the second harmonic of radio emission.
4. The radio flux of the burst attained $F = 10^3$ s.f.u.
5. The unusual burst was observed at a frequency as low as 1 MHz (STEREO/WAVES data).

We propose the following scenario of the generation of the caterpillar burst. The unusual burst was associated with active region NOAA1222 which started to be active at about 11:36 UT. The magnetic flux rope, which believed to be associated with this activity, propagated radially with a velocity of about 500 km s^{-1} away from the Sun. At heights $R = 2.22 - 2.55\,R_s$ the magnetic flux rope accelerated electrons. Moving towards and away from the Sun these particles generated the radio emission which was observed as the unusual radio burst. The particles propagating towards the Sun produced the radio emission with drift from low to high frequencies whereas particles moving away from the Sun generated the radio emission drifting from high to low frequencies. The velocities of the accelerated particles changed from $0.8 \cdot 10^9$ cm s^{-1} to $1.4 \cdot 10^9$ cm s^{-1} . At frequencies > 27.5 MHz the unusual burst was not observed because its radio emission could not propagate through the plasma of the solar corona towards the Earth.

Acknowledgements The work was partially fulfilled in the frame of FP7 project SOLSPANET (FP7-PEOPLE-2010-IRSES-269299). M. Panchenko acknowledges the Austrian Fond zur Foerderung der wissenschaftlichen Forschung (FWF projects P23762-N16).

Appendix

A. Propagation of the Radio Emission at the Second Harmonic from Behind-the-limb Region

Here we discuss the possibility for the radio emission at the second harmonic of local plasma frequency to propagate from the behind-the-limb region of the Sun towards the Earth. As was discussed in the present paper the unusual burst seems to be generated at the second harmonic of local plasma frequency. This

follows from low degree of polarization of the unusual radio burst which was about 10%. Note that the fundamental radio emission had higher degree of polarization (type IIIb bursts have 60-80%).

Let us discuss in detail the possibility to detect the radio emission at the second harmonic propagating from a behind-the-limb region by a ground-based radio telescope. Figure 13 presents the scheme of such propagation. The radio source is situated at a distance $R_{\rm H}$ from the solar center with the longitude α. The second harmonic can propagate towards the Earth if the distance $R_{\rm l}$ is larger than the distance $R_{\rm F}$. The last quantity corresponds to the radial distance at which the local plasma frequency $\omega_{\rm F}$ in the solar corona equals the double plasma frequency $\omega_{\rm H} = 2\omega_{\rm pe}$ at the place of generation of the second harmonic $\omega_{\rm F}(R = R_{\rm F}) = \omega_{\rm H}(R = R_{\rm H}) = 2\omega_{\rm pe}$. Therefore the condition for the observation of the behind-the-limb radio emission is

$$R_{\rm l} > R_{\rm F}. \tag{19}$$

In the opposite case, when $R_{\rm l} < R_{\rm F}$, the radio emission at the second harmonic cannot propagate towards the Earth.

In the case of the Newkirk model (Newkirk, 1961) of the solar corona, $n = n_{\rm N} \cdot 10^{4.32/r}$, where $n_{\rm N} = 4.2 \cdot 10^4$ cm^{-3} and $r = R/R_{\rm s}$, Equation (19) is satisfied when

$$R_{\rm H} > \frac{2.16}{\log 2}\left(\frac{1}{\cos\alpha} - 1\right) R_{\rm s}. \tag{20}$$

For the Baumbach-Allen model (Allen, 1947), $n = n_{\rm BA}(1.55r^{-6} + 2.99r^{-16})$, where $n_{\rm BA} = 10^8$ cm^{-3}, $r = R/R_{\rm s}$, we have

$$\cos\alpha > 2^{-1/3} \tag{21}$$

(for simplicity in the case of distances $r > 1.5$ we take into account only the first term, *i.e.* $n = n_{\rm BA} \cdot 1.55r^{-6}$). A similar result is obtained for the Leblanc model (Leblanc, Dulk, and Bougeret, 1998).

Therefore we can define the regions in the "frequency - longitudinal angle" plane where the radio emission at the second harmonic can propagate toward the Earth. In the case of the Baumbach-Allen model the emission can be detected at the Earth if the source is at the longitudinal angles $\alpha < 37.5°$. Moreover the radio emission can be observed in the whole frequency range (Figure 14, to the left from the dashed line).

If the coronal density follows the Newkirk model the higher possible frequency (or higher cut-off frequency) of the radio emission at the second harmonic detected at the Earth depends on the longitudinal angle α (Figure 14, solid line). Therefore in this case the radio emission can be observed in regions to the left of the solid line in Figure 14. This line is defined by

$$f^* = \frac{1}{\pi}\left(\frac{4\pi e^2 n_{\rm N}}{m_{\rm e}}\right)^{1/2} 2^{\cos\alpha/(1-\cos\alpha)} \tag{22}$$

where e and m_e is the charge and mass of the electron.

Assuming that the source of the unusual radio burst was related to active region NOAA1222, which was located at the longitudinal angles $40° - 50°$, and using Equation (20) we derive the distances at which the second harmonic emission can come out. These distances are $2.16 \cdot R_s$ (for $\alpha = 40°$) and $3 \cdot R_s$ (for $\alpha = 50°$). Maximal frequencies of the radio emission that are able to come out from these heights are 37 MHz and 12.7 MHz respectively. The cut-off frequency $f^* = 27.5$ MHz corresponds to the height $2.48 \cdot R_s$ is the highest frequency of the observed unusual radio burst.

References

Abranin, E.P., Bazelian, L.L., Rapoport, V.O., Tsybko, I.G.: 1980, Variations of type III burst parameters during a decametric solar storm. *Solar Phys.* **66**, 333 – 346. doi:10.1007/BF00150589.

Allen, C.W.: 1947, Interpretation of electron densities from corona brightness. *Mon. Not. Roy. Astron. Soc.* **107**, 426 – 432.

Bazelian, L.L., Zinichev, V.A., Rapoport, V.O.: 1978, Type III bursts with fine structure in the decameter range. *Radiofizika* **20**, 1399 – 1412.

Bougeret, J.L., Goetz, K., Kaiser, M.L., Bale, S.D., Kellogg, P.J., Maksimovic, M., Monge, N., Monson, S.J., Astier, P.L., Davy, S., Dekkali, M., Hinze, J.J., Manning, R.E., Aguilar-Rodriguez, E., Bonnin, X., Briand, C., Cairns, I.H., Cattell, C.A., Cecconi, B., Eastwood, J., Ergun, R.E., Fainberg, J., Hoang, S., Huttunen, K.E.J., Krucker, S., Lecacheux, A., MacDowall, R.J., Macher, W., Mangeney, A., Meetre, C.A., Moussas, X., Nguyen, Q.N., Oswald, T.H., Pulupa, M., Reiner, M.J., Robinson, P.A., Rucker, H., Salem, C., Santolik, O., Silvis, J.M., Ullrich, R., Zarka, P., Zouganelis, I.: 2008, S/WAVES: The radio and plasma wave investigation on the STEREO mission. *Space Sci. Rev.* **136**, 487 – 528. doi:10.1007/s11214-007-9298-8.

Brazhenko, A.I., Bulatsen, V.G., Vashchishin, R.V., Frantsuzenko, A.V., Konovalenko, A.A., Falkovich, I.S., Abranin, E.P., Ulyanov, O.M., Zakharenko, V.V., Lecacheux, A., Rucker, H.: 2005, New decameter radiopolarimeter URAN-2. *Kinematika i Fizika Nebesnykh Tel Suppl.* **5**, 43 – 46.

Briand, C., Zaslavsky, A., Maksimovic, M., Zarka, P., Lecacheux, A., Rucker, H.O., Konovalenko, A.A., Abranin, E.P., Dorovsky, V.V., Stanislavsky, A.A., Melnik, V.N.: 2008, Faint solar radio structures from decametric observations. *Astron. Astrophys.* **490**, 339 – 344. doi:10.1051/0004-6361:200809842.

Chernov, G.P., Stanislavsky, A.A., Konovalenko, A.A., Abranin, E.P., Dorovsky, V.V., Rucker, G.O.: 2007, Fine structure of decametric type II radio bursts. *Astron. Lett.* **33**, 192 – 202. doi:10.1134/S1063773707030061.

Dorovsky, V.V., Melnik, V.N., Konovalenko, A.A., Rucker, H.O., Abranin, E.P., Lecacheux, A.: 2010, Decametric solar U- and J-type bursts. *Radio Phys. Radio Astron.* **1**, 181 – 188. doi:10.1615/RadioPhysicsRadioAstronomy.v1.i3.10.

Dorovskyy, V.V., Melnik, V.N., Konovalenko, A.A., Rucker, H.O., Abranin, E.P., Lecacheux, A.: 2006, Observations of solar S-bursts at the decameter wavelengths. In: Rucker, H., Kurth, W., Mann, G., (ed.) *Planetary Radio Emissions VI*, Austrian Academy of Sciences Press, Vienna, 383 – 390.

Dorovskyy, V.V., Melnik, V.N., Konovalenko, A.A., Rucker, H.O., Abranin, E.P., Lecacheux, A.: 2011, Unusual type III bursts at the decametre wavelengths. In: Fischer, G., Kurth, W., Louarn, P., Rucker, H. (ed.) *Planetary Radio Emissions VII*, Austrian Academy of Sciences Press, Vienna, 359 – 366.

Dulk, G.A., Suzuki, S.: 1980, The position and polarization of type III solar bursts. *Astron. Astrophys.* **88**, 203 – 217.

Ginzburg, V.L., Zhelezniakov, V.V.: 1958, On the possible mechanisms of sporadic solar radio emission (radiation in an isotropic plasma). *Soviet Astron.* **2**, 653 – 678.

Konovalenko, A.A., Stanislavsky, A.A., Abranin, E.P., Dorovsky, V.V., Mel'Nik, V.N., Kaiser, M.L., Lecacheux, A., Rucker, H.O.: 2007, Absorption in burst emission. *Solar Phys.* **245**, 345 – 354. doi:10.1007/s11207-007-9049-8.

Kontar, E.P.: 2001, Dynamics of electron beams in the solar corona plasma with density fluctuations. *Astron. Astrophys.* **375**, 629 – 637. doi:10.1051/0004-6361:20010807.

Leblanc, Y., Dulk, G.A., Bougeret, J.-L.: 1998, Tracing the electron density from the corona to 1 AU. *Solar Phys.* **183**, 165 – 180. doi:10.1023/A:1005049730506.

Megn, A.V., Sharykin, N.K., Zaharenko, V.V., Bulatsen, V.G., Brazhenko, A.I., Vaschishin, R.V.: 2003, Decameter radio telescope URAN-2. *Radio Phys. Radio Astron.* **8**, 345 – 356.

Melnik, V.N., Kontar, E.P.: 2003, Plasma radio emission of beam-plasma structures in the solar corona. *Solar Phys.* **215**, 335 – 341. doi:10.1023/A:1025689116449.

Melnik, V.N., Konovalenko, A.A., Rucker, H.O., Stanislavsky, A.A., Abranin, E.P., Lecacheux, A., Mann, G., Warmuth, A., Zaitsev, V.V., Boudjada, M.Y., Dorovskii, V.V., Zaharenko, V.V., Lisachenko, V.N., Rosolen, C.: 2004, Observations of solar type II bursts at frequencies 10-30 MHz. *Solar Phys.* **222**, 151 – 166. doi:10.1023/B:SOLA.0000036854.66380.a4.

Melnik, V.N., Konovalenko, A.A., Dorovskyy, V.V., Rucker, H.O., Abranin, E.P., Lisachenko, V.N., Lecacheux, A.: 2005a, Solar drift pair bursts in the decameter range. *Solar Phys.* **231**, 143 – 155. doi:10.1007/s11207-005-8272-4.

Melnik, V.N., Konovalenko, A.A., Abranin, E.P., Dorovskyy, V.V., Stanislavsky, A.A., Rucker, H.O., Lecacheux, A.: 2005b, Solar sporadic radio emission in the decametre waveband. *Astron. Astrophys. Trans.* **24**, 391 – 401. doi:10.1080/10556790600568854.

Melnik, V.N., Konovalenko, A.A., Rucker, H.O., Rutkevych, B.P., Dorovskyy, V.V., Abranin, E.P., Brazhenko, A.I., Stanislavskii, A.A., Lecacheux, A.: 2008a, Decameter type III-like bursts. *Solar Phys.* **250**, 133 – 145. doi:10.1007/s11207-008-9166-z.

Melnik, V.N., Rucker, H.O., Konovalenko, A.A., Dorovskyy, V.V., Abranin, E.P., Brazhenko, A.I., Thide, B., Stanislavskyy, A.A.: 2008b, Solar Type IV Bursts at Frequencies 10-30 MHz. In: Wang, P. (ed.) *Solar Physics Research Trends*, Nova Science Publishers, New York, 287 – 325.

Melnik, V.N., Konovalenko, A.A., Brazhenko, A.I., Rucker, H.O., Dorovskyy, V.V., Abranin, E.P., Lecacheux, A., Lonskaya, A.S.: 2010a, Bursts in emission and absorption as a fine structure of Type IV bursts. In: Chakrabarti, S. K., Zhuk, A. I., Bisnovatyi-Kogan, G. S. (ed.) *Astrophysics and Cosmology after Gamow*, *AIP Conf. Proc.* **1206**, 450 – 454. doi:10.1063/1.3292553.

Melnik, V.N., Konovalenko, A.A., Rucker, H.O., Dorovskyy, V.V., Abranin, E.P., Lecacheux, A., Lonskaya, A.S.: 2010b, Solar S-bursts at frequencies of 10 - 30 MHz. *Solar Phys.* **264**, 103 – 117. doi:10.1007/s11207-010-9571-y.

Melnik, V.N., Rucker, H.O., Konovalenko, A.A., Shevchuk, N.V., Abranin, E.P., Dorovskyy, V.V., Lecacheux, A.: 2010c, Type IIIb bursts and their fine structure in frequency band 18-30 MHz. In: Chakrabarti, S. K., Zhuk, A. I., Bisnovatyi-Kogan, G. S. (ed.) *Astrophysics and Cosmology after Gamow*, *AIP Conf. Proc.* **1206**, 445 – 449. doi:10.1063/1.3292552.

Melnik, V.N., Shevchuk, N.V., Rucker, H.O., Konovalenko, A.A., Dorovskyy, V.V., Abranin, E.P., Lecacheux, A.: 2011, Properties of decameter spikes. In: Fischer, G., Kurth, W., Louarn, P., Rucker, H., (ed.) *Planetary Radio Emissions VII*, Austrian Academy of Sciences Press, Vienna, 351 – 358.

Newkirk, G. Jr.: 1961, The solar corona in active regions and the thermal origin of the slowly varying component of solar radio radiation. *Astrophys. J.* **133**, 983 – 1013. doi:10.1086/147104.

Ryabov, V.B., Vavriv, D.M., Zarka, P., Ryabov, B.P., Kozhin, R., Vinogradov, V.V., Denis, L.: 2010, A low-noise, high-dynamic-range, digital receiver for radio astronomy applications: An efficient solution for observing radio-bursts from Jupiter, the Sun, pulsars, and other astrophysical plasmas below 30 MHz. *Astron. Astrophys.* **510**, A16. doi:10.1051/0004-6361/200913335.

Suzuki, S., Dulk, G.A.: 1985, Bursts of type III and type V. In: McLean, D. J. Labrum, N. R. (ed.) *Solar Radiophysics: Studies of Emission from the Sun at Metre Wavelengths*, Cambridge University Press, Cambridge, 289 – 332.

Takakura, T., Yousef, S.: 1975, Type IIIb radio bursts - 80 MHz source position and theoretical model. *Solar Phys.* **40**, 421 – 438. doi:10.1007/BF00162389.

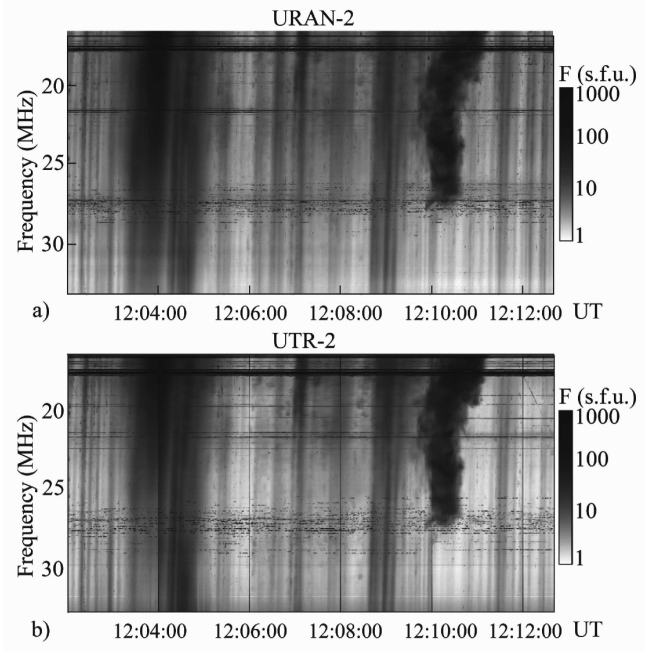

Figure 1. Unusual burst in the form of a caterpillar (12:10:00) observed by URAN-2 (a) and UTR-2 (b) against the background of a type III storm on 3 June 2011.

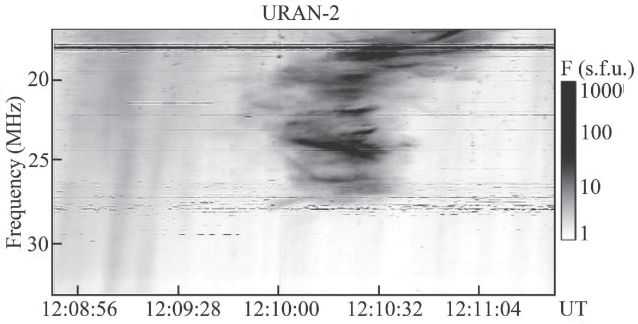

Figure 2. Fine structure in a form of horizontal stripes is well visible in the high resolution radio spectra of the unusual burst observed by URAN-2.

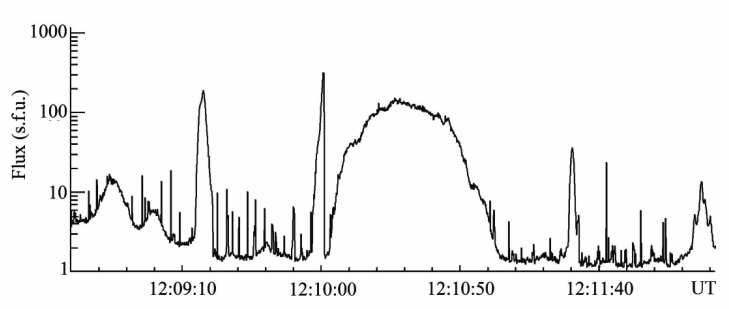

Figure 3. Time profile of the unusual burst at 26 MHz.

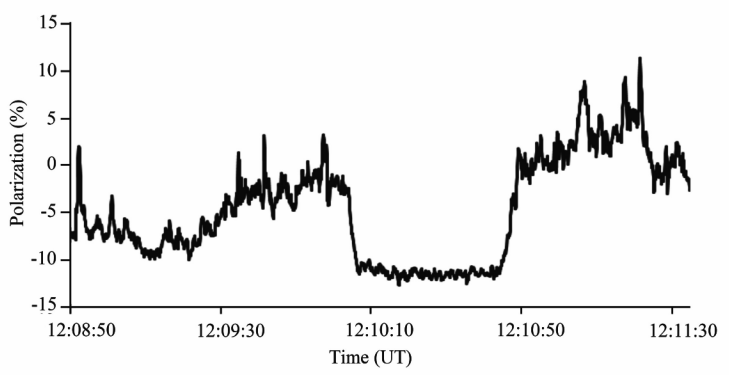

Figure 4. Polarization of the unusual burst at 26 MHz according to URAN-2 observations.

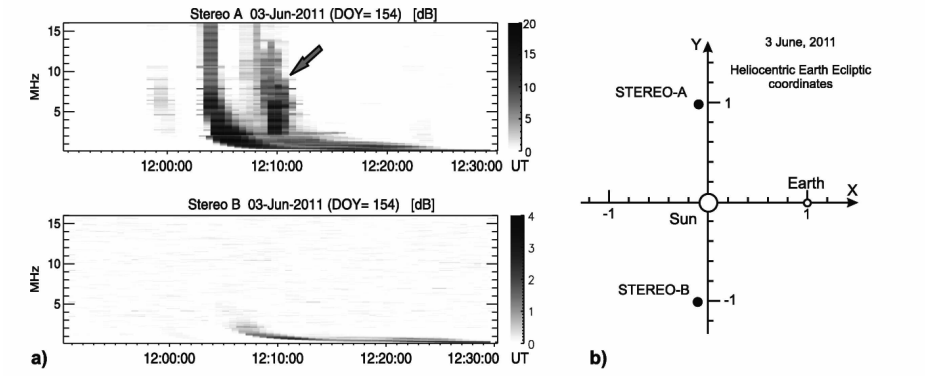

Figure 5. Radio spectra obtained by WAVES experiment onboard STEREO-A and STEREO-B on 3 June 2011 (panel (a)). The unusual solar radio burst was observed only by STEREO-A (marked by arrow). Panel (b) shows the positions of spacecraft in the heliocentric earth ecliptic coordinates.

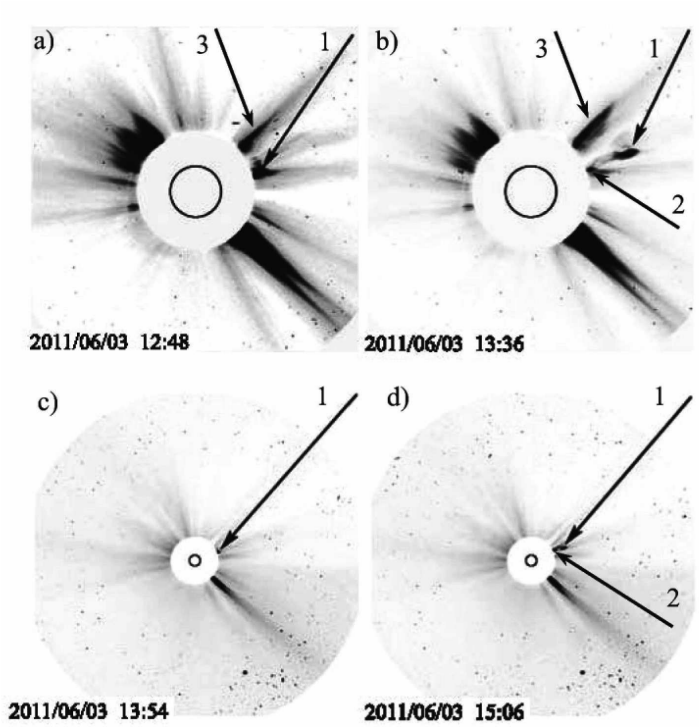

Figure 6. Two ejections (1 and 2) and jet (3) observed by LASCO C2 ((a), (b)) and by LASCO C3 (c), (d)) at the consistent moments of time.

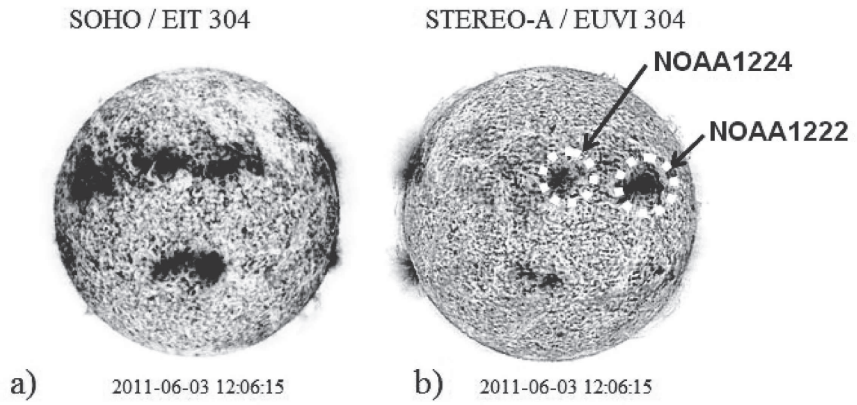

Figure 7. The solar disk with active regions observed by SOHO Extreme ultraviolet Imaging Telescope (SOHO/EIT 304Å) (a) and STEREO-A Extreme UltraViolet Imager (SECCHI EUVI) (b).

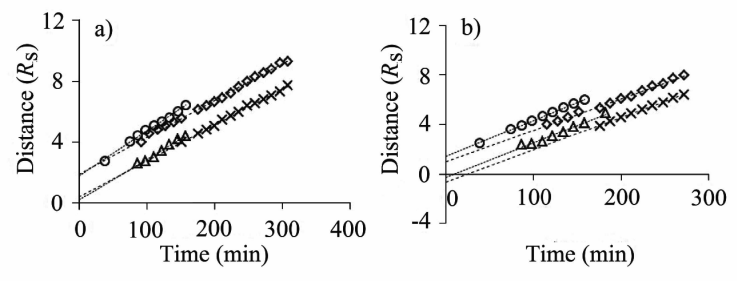

Figure 8. Motions of the front (a) and center (b) of ejections 1 (circles and rhombuses) and 2 (triangles and crosses). The time 0 in Figures 8-10 corresponds to 12:10 UT.

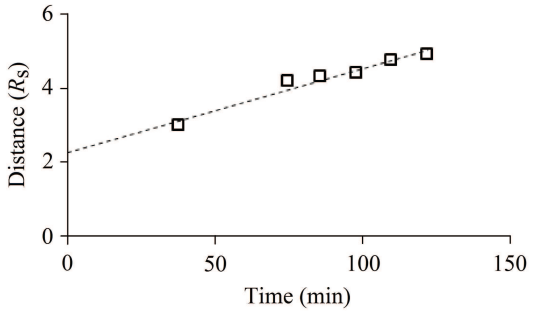

Figure 9. The motion of the jet front in the sky plane according to LASCO C2.

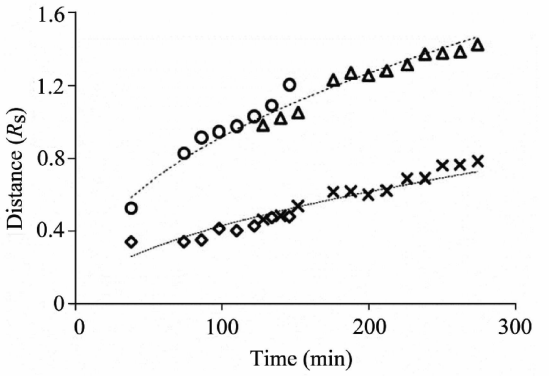

Figure 10. Longitudinal (circles and triangles) and transverse (rhombuses and crosses) sizes of the first ejection according to LASCO C2 and C3 data.

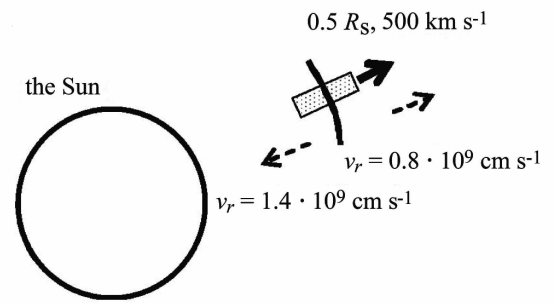

Figure 11. Scheme of the propagation of a magnetic flux rope in the solar corona.

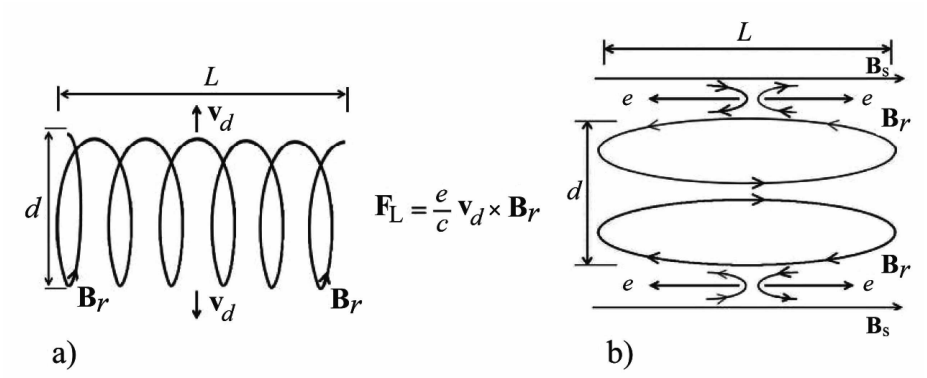

Figure 12. Acceleration of electrons by magnetic bunch due to the Lorenz force (a) and reconnection processes (b).

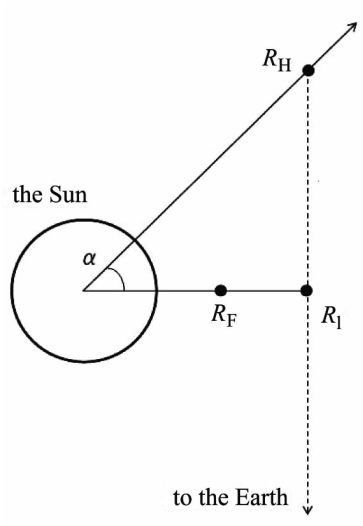

Figure 13. Scheme of propagation of radio emission at the second harmonic $\omega_H = 2\omega_{pe}$ (at altitude R_H) in the direction "towards the Earth" (latitudinal plane).

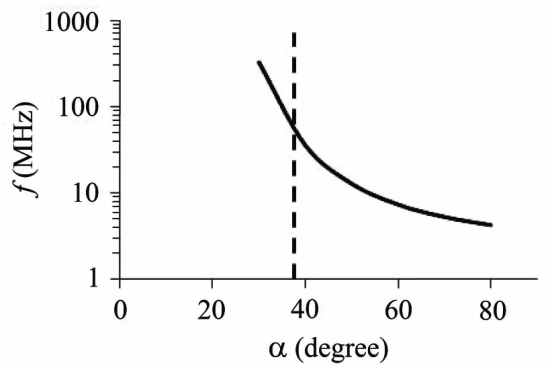

Figure 14. Regions of propagation of the second harmonic radio emission to the Earth from the "behind-the-limb" hemisphere in the Baumbach-Allen (dashed line) and Newkirk (solid line) models.